Available online at www.sciencedirect.com
ScienceDirect
Engineering Geology xx (2006) xxx–xxx
ENGINEERING GEOLOGY
www.elsevier.com/locate/enggeo

# Kinematics of a deep-seated landslide derived from photogrammetric, GPS and geophysical data

E. Brückl [a,*], F.K. Brunner [b], K. Kraus [c]

[a] Institute of Geodesy and Geophysics, Vienna University of Technology, Gußhausstrasse 27–29/E128, A-1040 Vienna, Austria
[b] Institute of Engineering Geodesy and Measurement Systems, Graz University of Technology, Steyrergasse 30/II, A-8010 Graz, Austria
[c] Institute of Photogrammetry and Remote Sensing, Vienna University of Technology, Gußhausstrasse 27–29/E122, A-1040 Vienna, Austria

Accepted 11 September 2006

**Abstract**

The deep-seated landslide located at the intersection of the Gradenbach and Möll valleys near Döllach, Austria, has been the target of many previous investigations [Kronfellner-Kraus, G., 1980. Neue Untersuchungsergebnisse in Wildbächen — Der Talzuschub in Abhängigkeit von Niederschlägen. Int. Symp. Interpraevent Bad Ischl 1: 179–192; Weidner, S., Moser, M., Lang, E., 1998. Influence of hydrology on sagging of mountain slopes ("Talzuschübe") — New results of time series analysis. 8th International IAEG Congress, Vancouver, Canada, Balkema, Rotterdam, 1259–1266; Weidner, S., 2000. Kinematik und Mechanismus tiefgreifender alpiner Hangdeformationen unter besonderer Berücksichtigung der hydrologischen Verhältnisse. Dissertation, Friedrich–Alexander-Universität Erlangen–Nürnberg, 246.]. In this paper, photogrammetric, GPS and geophysical data have been utilized to derive a constraint on the kinematics of the sagging process. The photogrammetric models have been based on aerial photographs from 1962 and 1996. Displacement vectors of about 50 individual characteristic points have been determined; these clearly show the area of the sagging slope. From 1999 to 2004, eleven GPS campaigns have been carried out, yielding very accurate displacement vectors at four monitoring points. Information about the internal structure of the slope was determined using seismic surveys.

The displacements observed by photogrammetry and GPS have shown a rather uniform movement of the whole sagging slope, with a slight longitudinal compression of 0.6%. In order to extend the kinematic consideration to 3D, a special form of the equation of continuity (conservation of mass) has been applied to the 1962–1996 photogrammetric data, together with the cross-sections derived from the seismic data. The average velocities through cross-sections have been calculated by integrals of the mass-balance above and below these cross-sections. Changes of the total rock mass, due to accumulation and especially to erosion, as well as an overall compaction of 1.5% between 1962 and 1996, have been considered. The calculated average velocities through a cross-section and the surface velocities independently determined by photogrammetry agree within an uncertainty of 15%. The results indicate a block movement with shear concentration at the basal sliding surface.


*Keywords:* Deep-seated gravitational creep; Sagging; Landslide; Photogrammetry; GPS; Geophysics; Kinematics

## 1. Introduction

Landslides, which are unavoidable natural processes in alpine regions, have often been associated with economic and social disasters. Therefore, the prediction

* Corresponding author. Tel.: +43 1 58801/12820; fax: +43 1 58801/12892.
*E-mail address:* ebrueckl@luna.tuwien.ac.at (E. Brückl).

0013-7952/$ - see front matter © 2006 Elsevier B.V. All rights reserved.
doi:10.1016/j.enggeo.2006.09.004

of landslides has become a key issue in natural disaster reduction. As a consequence, large efforts have been made to investigate the causes and mechanisms of landslides. This paper has concentrated on the kinematics of deep-seated mass-movements.

On alpine slopes, deep-seated gravitational creep is a frequently observed phenomenon (e.g., Bisci et al., 1996). The deformation pattern, which looks like the gravitational slumping of a sack, inspired Zischinsky (1969) to coin the term "sagging" (Sackung). The rock material forming sagging slopes is best described as brittle rock. The volume of the creeping rock mass is usually about $10^8$ $m^3$ or larger. The surface velocities vary from millimetres to metres per year and may significantly change with time. Although the movements are known to be influenced by precipitation and groundwater level variations, modelling these effects has been rather difficult.

Seismic surveys provide information about the thickness of a sagging slope, whilst geodetic deformation surveys produce maps of average motions of the surface of the slope. The fusion of these data, through the equation of conservation of mass, yields information about the variation of the velocity with depth. The development of this model will be explained and applied to data sets (photogrammetric surveys and GPS monitoring) of the Gradenbach deep-seated mass-movement. It has been shown that an interpretation of the kinematics of the Gradenbach sagging based on this data fusion, yields important information for estimating the potential for hazards.

## 2. Study area

The Gradenbach deep-seated mass-movement is situated at the junction of the Graden and the Möll valleys (Carinthia, Austria), about 7 km to the south of Heiligenblut (see inset in Fig. 1). The active deformation zone is located at the southeast side of the Eggerwiesenkopf near the hamlet of Putschall (see Fig. 1). It involves an area of about 1.7 $km^2$, with width ranging between 600 and 1000 m, and an extent of approximately 1000 m in height, from the head scarp at 2270 m down to the slide toe, at a height between 1100 and 1270 m (Fig. 1). The clearly developed head scarp lies slightly below the mountain ridge and has a lateral extent of about 40 m (Fig. 2). Phyllites and calcareous schists (Matrei zone), which were severely stressed during the Alpine orogenesis, are predominately found in the active deformation zone.

For the past 30 years, the Gradenbach landslide has been extensively investigated because of its interesting geotechnical aspects (Weidner et al., 1998). The mass-movement accelerated in 1965 and 1966, triggering catastrophic debris flows which devastated the hamlet of Putschall. At irregular intervals between 1969 and 1991 (Kronfellner-Kraus, 1980) geodetic (terrestrial) measurements have been carried out. Using this data, the average slope displacement rate has been estimated at about 10 cm/yr (Weidner, 2000). From 1969 to 1991, the average horizontal displacement in the upper part of the sagging mass was 11.9 m, and at the toe zone 7.4 m (Weidner et al., 1998).

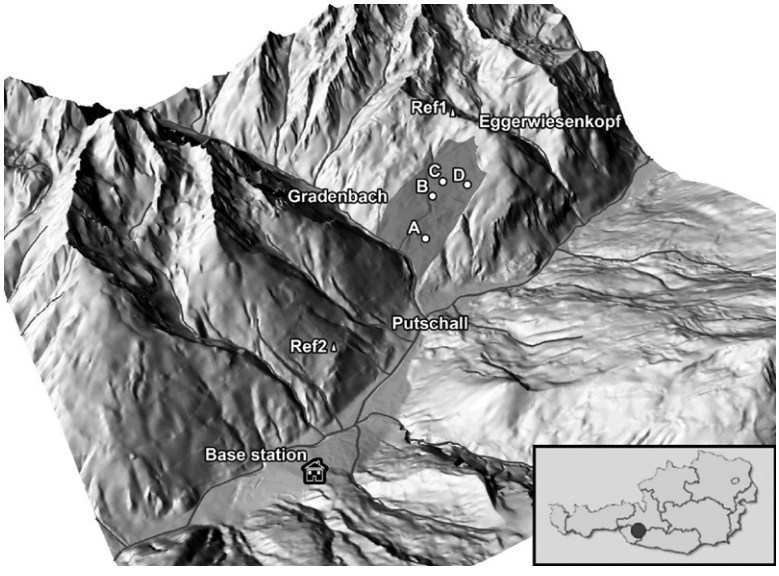


Fig. 1. Topography of the Gradenbach landslide area: all GPS stations of the monitoring network are shown. For scale estimation: the horizontal distance between Ref 2 and A is 2600 m.

Please cite this article as: E. Brückl et al., Kinematics of a deep-seated landslide derived from photogrammetric, GPS and geophysical data, Engineering Geology (2006), doi:10.1016/j.enggeo.2006.09.004

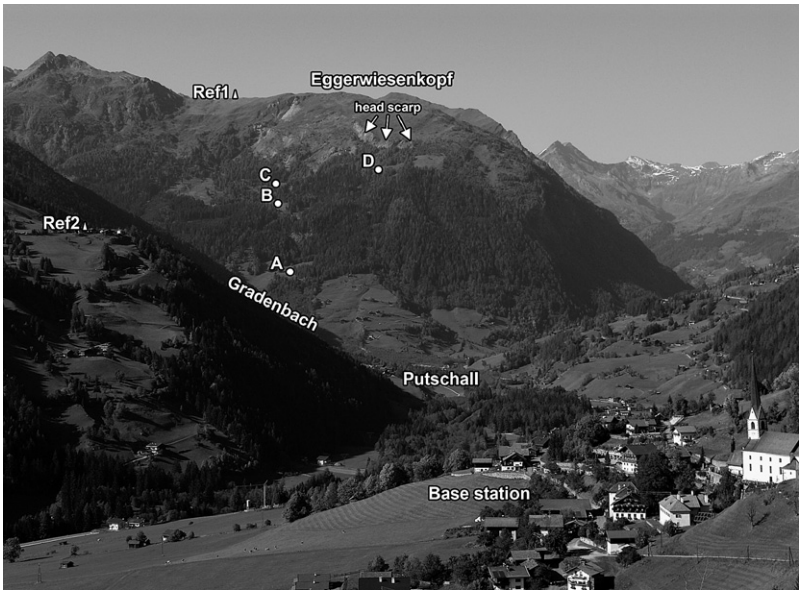


Fig. 2. Gradenbach landslide, head scarp, GPS stations Ref 1, Ref 2, A, B, C and D.

The base of the creeping rock mass is here called the basal surface. This has been derived from 5 refraction seismic lines and two boreholes which reached coherent rock below the mass-movement (Brückl and Brückl, 2006). Area and volume of the mass-movement are $1.68\ 10^6$ m$^2$ and $121\ 10^6$ m$^3$, respectively. The uncertainty of the volume estimate is about 15%. An average porosity of the creeping rock mass $n=28\%$ was estimated by a correlation with the seismic velocities (Watkins et al., 1972).

## 3. Photogrammetric measurements

### 3.1. General remarks

Since about 1950, stereoscopic aerial photographs have been taken of wide areas of Austria, thus offering the possibility for monitoring geomorphological processes during the past 50 years. The accuracy of photogrammetric measurements mainly depends on the flying height. Nowadays, with a very low flying height it is possible to achieve centimeter accuracy for points on the ground. However, with the flying height and the photographic quality of older projects, like those in the Gradenbach area, an accuracy no better than in the range of metres is obtained.

Despite the relatively low photogrammetric accuracy of individual points, morphological models may be derived with a significantly better accuracy. Photogrammetric methods deliver a great number of individual point measurements, from which the irregular part, i.e. the noise, may be removed if they are combined to one morphometric model — provided the model needs only a small number of parameters. Such a noise elimination process is also referred to as filtering.

For the Gradenbach project various photogrammetric measuring, modeling and analysing procedures have been employed. Terrain models have been generated in order to derive the geomorphological shape. In addition digital orthophotos have been created and 3D motion vectors determined at selected points. Similar projects, comparable to a certain extent, may be found in Casson et al. (2003) and Kääb (2002). For the Gradenbach project aerial photographs of the years 1962 and 1996 have been used, whose technical specifications are listed in Table 1.

### 3.2. Digital terrain models and their changes

3D coordinates have been determined for all points, which have been confidently identified in overlapping areas of adjacent photographs (an overlap of some 60% of neighbouring images is usual). The object coordinate

Table 1
Specifications of the aerial photographs

| Year | Absolute flying height | Principal distance | Image format | Film |
|---|---|---|---|---|
| 1962 | 4400 m | 210 mm | 18 × 18 cm | Black-and-white |
| 1996 | 6100 m | 208 mm | 23 × 23 cm | Colour infrared |

Please cite this article as: E. Brückl et al., Kinematics of a deep-seated landslide derived from photogrammetric, GPS and geophysical data, Engineering Geology (2006), doi:10.1016/j.enggeo.2006.09.004

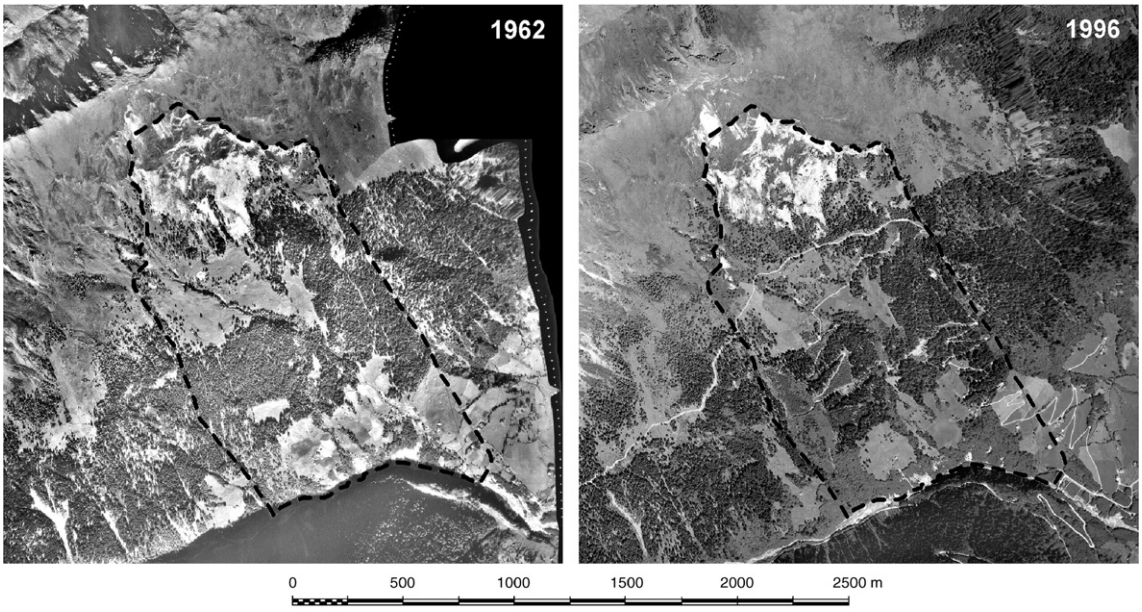


Fig. 3. Orthophotos of 1962 (left) and 1996 (right).

system, also referred to as the reference system, may be fixed in space with the help of several ground control points whose coordinates can be measured by terrestrial techniques. Matching of image points with their homologous partners in the neighbouring image can be done automatically by digital image correlation (e.g., Kääb, 2002), although reliable and satisfying results can be achieved in scarcely vegetated areas only. As the Gradenbach region is covered by relatively dense forest (Fig. 3), matching of homologous points has been carried out by a human operator through stereo measurements. From the images of the 1962 flight, 7732 points and from those of the 1996 flight 8100 points have been measured. Additionally, 3D breaklines, i.e. terrain discontinuities, have been digitized.

From each of the point clouds from 1962 and 1996, a digital terrain model (DTM) has been derived with a grid width of 2.5 m. The linear prediction algorithm (Kraus and Pfeifer, 1998), which is related to the Krige estimator (Kraus, 2000; Isaaks and Srivastava, 1990) was used. The average magnitude of the discrepancies between the original points and the DTM, i.e. the mean filter value was ±0.49 m for the 1962 DTM and ±0.26 m for the 1996 DTM.

Since the same ground control points have been used for georeferencing both the DTM 1962 and DTM 1996, and since these points were not affected by any ground motion, the comparison of the DTMs delivers the volume change for each cell of the regular grid. Fig. 4 shows the elevation differences of the terrain surfaces between 1962 and 1996. The integral over these differences yields a volume decrease of 2.8 $10^6$ $m^3$ for this period.

### 3.3. Digital orthophotos

Aerial photographs have to be georeferenced with the help of ground control points and a DTM (e.g., Kraus, 1997). Using this information, a digital orthophoto can be produced (Kraus, 1997). Fig. 4 shows the digital

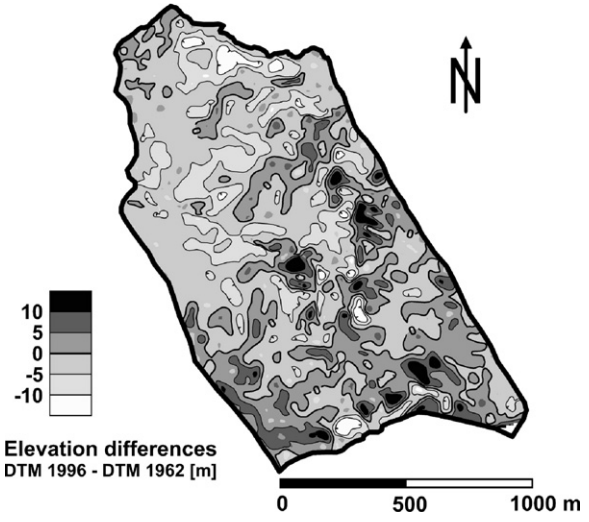


Fig. 4. Elevation differences from a comparison of the DTM 1996 and the DTM 1962.

Please cite this article as: E. Brückl et al., Kinematics of a deep-seated landslide derived from photogrammetric, GPS and geophysical data, Engineering Geology (2006), doi:10.1016/j.enggeo.2006.09.004

orthophotos of the 1962 flight (left) and the 1996 flight (right). For both orthophotos, a ground sampling distance of 0.25 m was used.

If both orthophotos are superimposed on a computer screen, the changes between the two epochs can clearly be recognised. The boundary between the stable and moving parts of terrain can be determined by comparing the 1962 and 1996 orthophotos, although orthophotos only show horizontal displacements. The horizontal displacements at homologous points can only be determined through manual observation because of the rather large differences between both orthophotos and the heavy changes of vegetation within a 34 year time span between the photographs. If the photo texture had been very similar for the two epochs, then digital correlation techniques could have been used (e.g., Kääb, 2002).

### 3.4. Three dimensional motion vectors

Photogrammetry is a three dimensional measurement process. It is, therefore, best suited for the determination of 3D motion vectors. The major problem is finding homologous points in the stereo images of different epochs. The problem becomes even more difficult as the motion vectors become larger, and the more different the surface textures appear in the two images. The Gradenbach area is especially difficult to analyse, as can be seen from the orthophotos (Fig. 3).

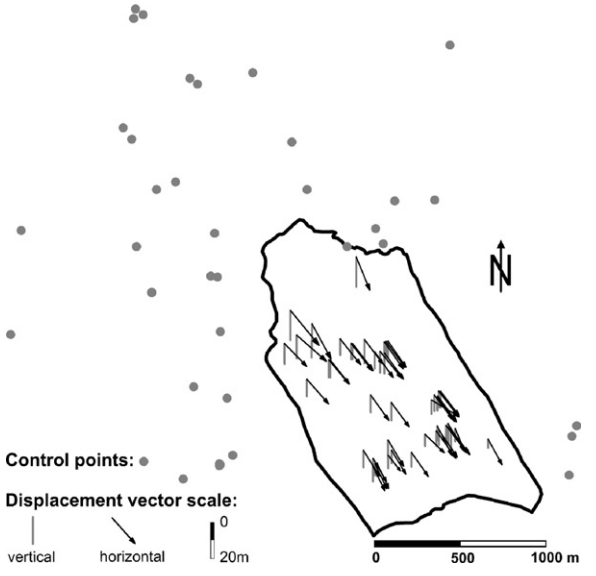


Fig. 5. Displacement vectors for the 1962–1996 period, derived from photogrammetric measurements; horizontal components (right), vertical components (left).

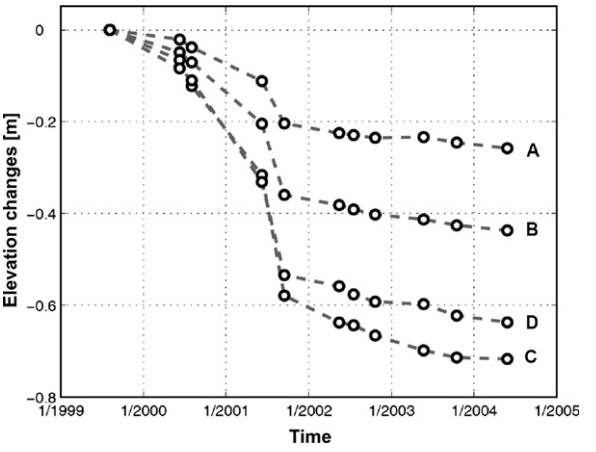


Fig. 6. Vertical motions of GPS monitoring points A to D; circles indicate the GPS campaigns.

Even under these difficult circumstances, the following strategy leads to satisfying results: At the beginning the operator chooses a great number of suspected homologous points in the stereo images of the two epochs, even if there is some doubt of their identity. The differences of the 3D coordinates between the two epochs are the components of the 3D motion vectors. Thereafter these discrete 3D motion vectors are input into a procedure for creating a (continuous) displacement model. By combining the individual point measurements in this way, methods of geostatistical analysis may help, firstly, to filter out the stochastic measurement errors (i.e., noise) of the individual measurements and, secondly, to detect blunders, that is, errors in matching homologous points (Kraus, 2000).

In the Gradenbach project, 120 3D motion vectors have been measured photogrammetrically for the period 1962–1996. Moreover, 35 points had vectors with a length significantly below the measuring noise. These points have been classified as further control points, in addition to those mentioned in Section 3.2. All these points served as the frame for the reference coordinate system for the motion measurements. The remaining 85 motion vectors had to undergo a blunder detection procedure, during which about 10% of the data were eliminated. An additional data reduction has been carried out by averaging closely spaced displacement vectors. The final set of 51 vectors is shown in Fig. 5, separated into horizontal and vertical components. These motion vectors may serve as a supplementary check on whether the boundary between the moving and stable areas has been selected correctly in the orthophotos (Section 3.3). The compilation of the photogrammetric measurements has been accomplished with

Please cite this article as: E. Brückl et al., Kinematics of a deep-seated landslide derived from photogrammetric, GPS and geophysical data, Engineering Geology (2006), doi:10.1016/j.enggeo.2006.09.004

the help of the bundle adjustment program ORIENT, which contains many statistical tests, including Data Snooping (Kraus, 1997).

The geostatistical analysis of the motion vectors (Kraus, 2000) within the landslide region yielded a stochastic part of 2.9 m for a horizontal component, and 2.1 m for a vertical component.

## 4. GPS measurements

### 4.1. Measurement system

The advantage of GPS measurements in comparison to optical surveying measurements are the high accuracy potential especially for large areas, the weather independence, and the fact that no line-of-sight observations between the stations are necessary. The technique to achieve highly accurate GPS measurements is based on the use of GPS signals differenced between two stations and two satellites. If the coordinates of one station (reference) are well known, then the coordinates of the second station (monitoring) can be computed with high accuracy.

An autonomous GPS monitoring system has been developed for the investigation of landslides (Brunner et al., 2003). In its current configuration, the monitoring system consists of six GPS stations, at least two of which are used as reference for the remaining monitoring stations. The system could easily be extended to more than six stations. The GPS hardware at a station consists of a choke-ring antenna with a radome protection and a GPS receiver. The GPS data are transferred to a central computer by radio, where the data are stored and immediately processed. Power supplies and lightning protection were developed for the autonomous operation.

The software GRAZIA has been developed for processing the GPS measurements, with special attention given to data quality issues. GRAZIA computes the coordinate results from all observed GPS phase values in a so-called network solution. It is possible to use several reference stations simultaneously. The original phase data are “cleaned”, and then properly weighted, using the observed signal-to-noise ratio values (Wieser and Brunner, 2002). The tropospheric propagation effects can produce large but “fake” height variations. Thus an appropriate correction module has been developed. The effectiveness of these processing modules, especially for the case when large height differences are surveyed, was discussed by Brunner et al. (2003). Standard GPS techniques, as investigated by Mora et al. (2003) for landslide studies, would yield inferior accuracies.

### 4.2. Campaigns and results

The Gradenbach mass-movement was surveyed using eleven measurement campaigns during the past five years. For the GPS network, two reference stations were selected in the stable bedrock area: Ref 1 at the mountain ridge of the Eggerwiesenkopf, at a height of 2270 m, and Ref 2 on a glacial rock terrace on the opposite slope, at a height of 1400 m (Figs. 1 and 2). The four monitoring points (A to D) situated in the active part of the slope were selected to form approximately a straight line between the two reference stations. The first GPS survey (zero-measurement) took place in August 1999. The results of all following campaigns refer to this zero-measurement, for which GPS data were recorded during 48 h. Since then, every year at least two measurement campaigns took place. A session length of 48 h was chosen in order to further reduce periodic (especially diurnal) effects on the GPS results.

In addition, several continuous measurement campaigns were carried out (not shown in Fig. 6). These results were used to estimate the attainable precision: horizontal position differences (relative to the reference stations) have a precision of 4 mm, with a precision of 7 mm for the height determinations. The latter value is

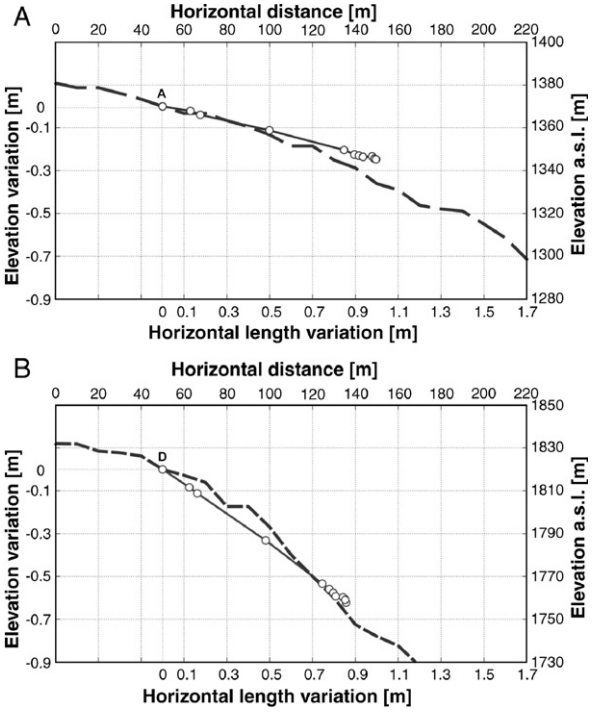


Fig. 7. Horizontal and vertical displacements derived from GPS results (circles), and cross-section of the topography in the dip direction of the slope for the monitoring stations A (A) and D (B).

Please cite this article as: E. Brückl et al., Kinematics of a deep-seated landslide derived from photogrammetric, GPS and geophysical data, Engineering Geology (2006), doi:10.1016/j.enggeo.2006.09.004

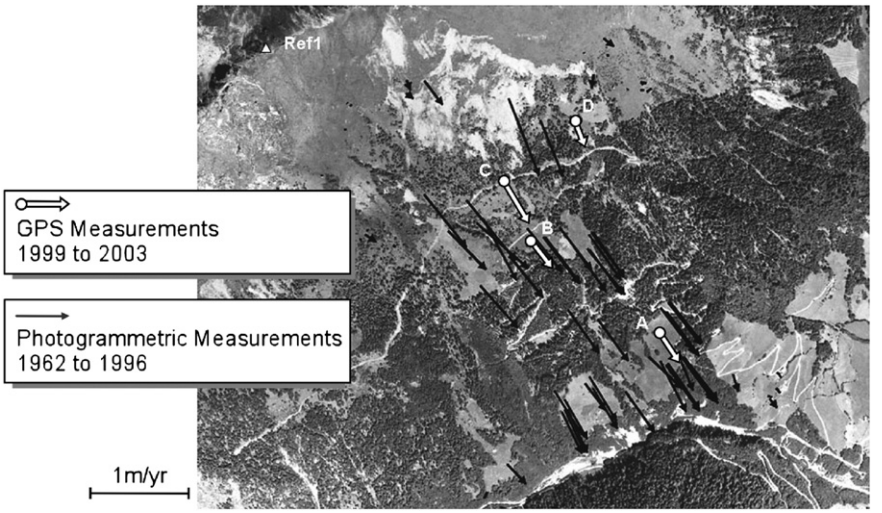


Fig. 8. Comparison of horizontal displacement rates (average values in m/yr) obtained by photogrammetry and GPS.

due to the effectiveness of the new tropospheric model, which uses Ref 2 for the calibration of the tropospheric propagation effects. More details on this method have been presented by Brunner et al. (2003).

All coordinate results obtained since the zero-measurement in August 1999 have been used to investigate the landslide motion during the following years. Fig. 6 shows the vertical motions of the four monitoring points, all referred to the zero-measurement results. The vertical motions show a continuous acceleration until September 2001, but afterwards the motion rate decreased suddenly. The following quiescent period has continued up to the present day (November 2004).

The azimuths of the observed displacements coincide approximately with the dip direction of the slope. Fig. 7A and B show the horizontal and vertical displacements of the monitoring stations A and D superimposed on the cross-sections of the topography around these stations in the direction of movement. The vertical displacement components increase significantly with station elevation.

During the period 1990–2000, geotechnical and also terrestrial geodetic measurements indicated a decrease of the motion rate for the landslide. The annual average was about 0.11 m/yr (Weidner, 2000). However, the GPS measurements showed a motion rate of 0.15 to 0.30 m/yr between 1999 and 2000 and a dramatic acceleration up to September 2001, resulting in a 50 cm motion during three months (this would correspond to 2 m/yr). After this event, the movement rate slowed down (Fig. 6). Future GPS measurements should clarify the geomechanics of the slope resulting in periods of accelerated motions followed by quiescent periods.

## 5. Kinematics

### 5.1. Comparison of photogrammetric and GPS data

The photogrammetric and GPS results of the previous two sections are derived using completely independent techniques. Note that an additional photogrammetric flight covering the Gradenbach area was carried out in 2003; the images have not yet been released for processing. It will certainly be interesting to produce deformation vectors by the photogrammetric technique for the period 1996 to 2003 and compare the results with the deformation values derived by GPS monitoring for essentially the same period.

The photogrammetric results yield average values for the displacement rates between 1962 and 1996; this period includes the catastrophic motions which occurred in 1965/66 (Kronfellner-Kraus, 1980). Fig. 8 shows the horizontal displacement rates for all photogrammetric measurements. GPS monitoring yields precise displacement rates at four stations only and for a different time

Table 2
Comparison of horizontal and vertical displacements derived from photogrammetric (1962–1996) and GPS (1999–2003) measurements and the appropriate ratios

| Stations | Length (hor.) | | | Height | | |
|---|---|---|---|---|---|---|
| | Photo. m | GPS m | Ratio | Photo. m | GPS m | Ratio |
| A | 17.8 | 1.016 | 17.5 | −8.7 | −0.258 | 33.7 |
| B | 19.4 | 1.153 | 16.8 | −10.6 | −0.437 | 24.3 |
| C | 21.8 | 1.589 | 13.7 | −13.6 | −0.717 | 19.0 |
| D | 16.8 | 0.876 | 19.2 | −12.3 | −0.637 | 19.3 |

Please cite this article as: E. Brückl et al., Kinematics of a deep-seated landslide derived from photogrammetric, GPS and geophysical data, Engineering Geology (2006), doi:10.1016/j.enggeo.2006.09.004

period than the photogrammetric results. Comparing the orientations of the average displacement vectors in Fig. 8, reveals a very high consistency for the two nearly consecutive periods. This indicates that the kinematics of the sagging is controlled by the same structures and processes over both periods of observation (photogrammetry and GPS). However, the average lengths of the displacement vectors vary slightly with elevation (see also Fig. 7) and time. For an at least spatially correct comparison, the photogrammetric results were interpolated with the displacement model of Section 3.4 to the positions of the four GPS monitoring points (Table 2). The ratios of the horizontal displacement components calculated from photogrammetry and GPS vary from 13.7 to 19.2 and do not show a significant variation with elevation. The corresponding ratios for the vertical components at stations C and D, located on the upper part of the slope are 19.0 and 19.3, which is nearly in the range of the ratios for the horizontal displacements. This indicates a similar kinematics at stations C and D during the 1962–1996 (photogrammetric observations) and 1999–2003 (GPS observations) periods. In the lower part of the slope, at the stations A and B, the ratios are significantly higher (24.3 and 33.7). These higher ratios of the vertical component may be interpreted as caused by a small-scale rotational movement or by a compaction process during the 1962–1996 period; this is further discussed below. In general, the creep velocity was two times higher during 1962–1996 than during 1999–2003.

The analysis of historic photogrammetric flights produces invaluable information about the past development of a mass-movement. It can produce 3D displacement vectors between the epochs of the flights for as many homologous points as can be identified (Section 3.4). An additional advantage is that no new fieldwork is required. GPS monitoring is applicable to current landslide motion studies only; the GPS stations can be placed

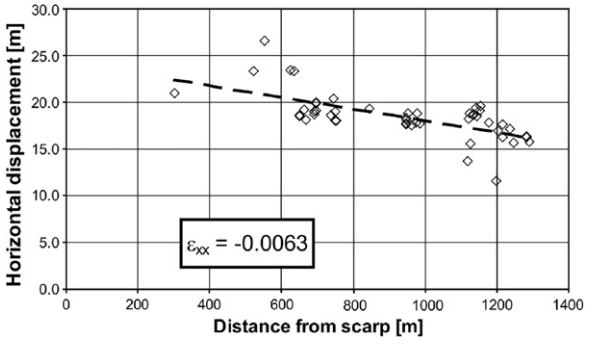


Fig. 9. Longitudinal strain derived from photogrammetric data.

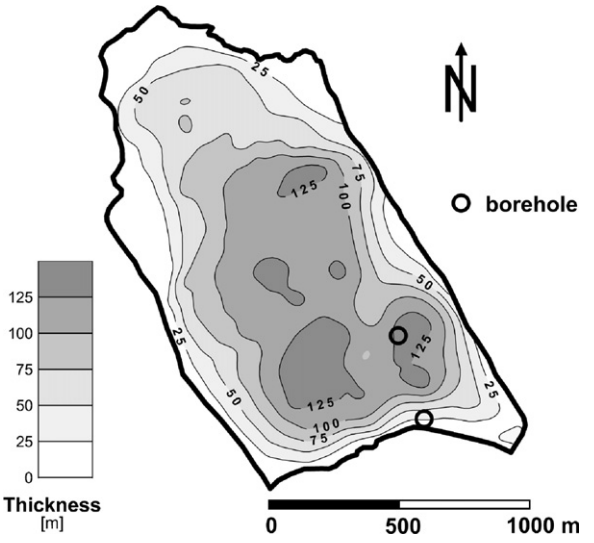


Fig. 10. Thickness of the creeping rock mass derived from seismic refraction data and two boreholes.

at desirable points in the field, and the attainable precision is in the millimetre range. The time resolution of the landslide motions only depends on the frequency of the GPS measurements. The great advantage of GPS monitoring is highlighted in Fig. 6, where the recent acceleration and deceleration cycle of the Gradenbach landslide has been shown. The kinematics of this rather typical cycle of acceleration followed by sudden deceleration is currently being investigated.

### 5.2. Deformation derived from surface measurements

Several kinematic quantities can be derived from photogrammetric and geodetic surface measurements alone. As pointed out in Section 3.2, the volume of the moving rock mass decreased by 2.8 $10^6$ $m^3$ from 1962 to 1996. About 1.0 $10^6$ $m^3$ can be attributed to erosion by the river at the toe of the slope. In order to estimate the amount of erosion, the area of the near vertical front of the mass-movement was determined by photogrammetric observations. No significant change in the area of the front was detected. Therefore, the erosion is the scalar product of this area and the displacement. The displacement was extrapolated from nearby photogrammetric observations. The remaining volume decrease of 1.8 $10^6$ $m^3$ is interpreted as compaction by 1.5% of the creeping rock mass. The accuracy of the determination is not sufficient to distinguish between the regions of higher and lower compaction. In general one would expect a progressive disintegration and an increase in porosity of the creeping rock mass with ongoing

Please cite this article as: E. Brückl et al., Kinematics of a deep-seated landslide derived from photogrammetric, GPS and geophysical data, Engineering Geology (2006), doi:10.1016/j.enggeo.2006.09.004

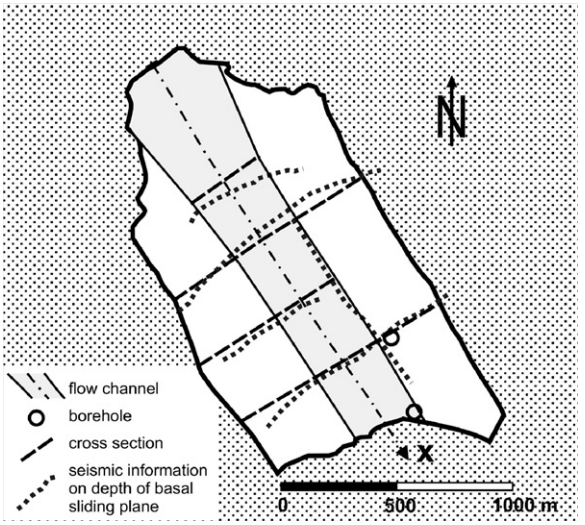


Fig. 11. Partitioning of the mass-movement into flow channels cut by representative cross-sections.

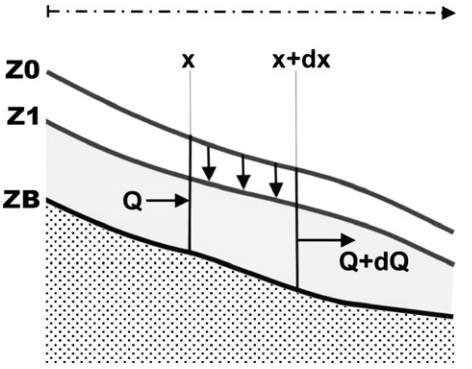


Fig. 12. Longitudinal section through the mass-movement showing the relation between change of elevation and increment of flux. $Q$ incoming flux of rock mass through the cross-section at $x$, $Q+\mathrm{d}Q$ outgoing flux of rock mass through the cross-section at $x+\mathrm{d}x$, Zs0, Zs1 elevations at $T0$ (1962) and $T1$ (1996), Zb elevation of the basal plane.

movements. Therefore the compaction of 1.5% derived for the period from 1962 to 1996 should be considered as transient only.

Fig. 9 shows the horizontal displacement over $x$, a curvilinear centre flow line. A significant decrease in the displacement with distance downslope can be observed. The mean longitudinal strain of the moving rock mass is about $e_{xx}=-0.006$. From this, it can be concluded that the lower part of the slope supports the rock mass sagging down from the upper part. However, the longitudinal compression explains only 40% of the total compaction of 1.5%.

### 5.3. Mass flow

The differences between the elevations of the DTM 1996 and the DTM 1962 (Fig. 4) give a first impression of the mass-flow from the upper to the lower part of the slope during this time span. These changes, termed "mass balance" for simplicity, are related to the horizontal component of the average velocity by the equation of continuity, which has been successfully applied to glacial flow for nearly a century (Finsterwalder, 1907; Nye, 1963). Recently, this idea was adapted to studies of the mass-flow of saggings used in connection with the reconstruction of the pre-failure topography of the sagging slope (Brückl and Brückl, 2006). Besides the mass-balance, the thickness of the creeping rock mass must also be known in order to calculate velocities. The thickness map derived from two boreholes and 5 refraction seismic lines is shown in Fig. 10. The locations of points at the basal plane where either seismic or borehole information is available are shown in Fig. 11. More information about the seismic exploration of the Gradenbach sagging is provided by Brückl and Brückl (2006).

The creeping rock mass is considered to be divided into several flow channels confined by flow lines. The actual subdivision into flow channels and representative cross-sections is shown in Fig. 11. Changes of the elevation of the basal surface between 1962 and 1996 are neglected and erosion is considered only at the toe of the slope according to the photogrammetric results. For

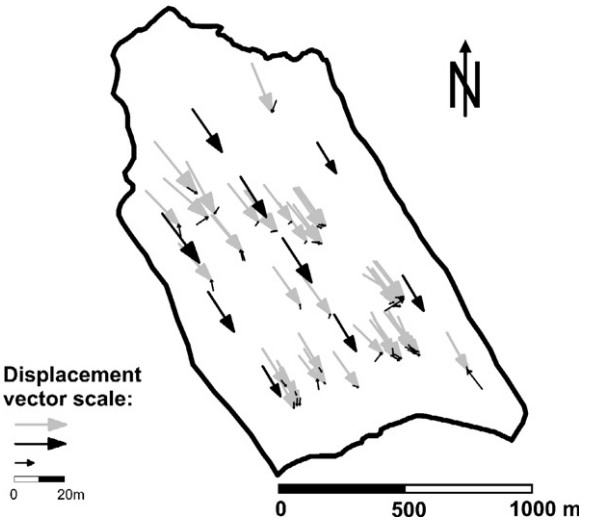


Fig. 13. Comparison of calculated average displacements (bold black arrows) and observed surface displacements (bold grey arrows); thin black arrows show the difference.

Please cite this article as: E. Brückl et al., Kinematics of a deep-seated landslide derived from photogrammetric, GPS and geophysical data, Engineering Geology (2006), doi:10.1016/j.enggeo.2006.09.004

this simpler case, the equation of continuity can be derived from the longitudinal-section shown in Fig. 12.

$$dQ \cdot (T1-T0) = (1-n1) \cdot (Zs0-Zs1) \cdot B \cdot dx + \Delta n \cdot (Zs0-Zb) \cdot B \cdot dx \quad (1)$$

$Q$ …flux $Q$ at $x$
$dQ$ …increment of flux $Q$ between $x$ and $x+dx$
$T0$, $T1$…date of first (1962) and second (1992) photogrammetric mapping
$n1$ …porosity at $T1$
$\Delta n$ …change in porosity between $T1$ and $T0$
Zs0, Zs1…elevations at $T0$ and $T1$ at $x+dx/2$
Zb …elevation of basal surface at $x+dx/2$
$B$ …width of flow channel at $x+dx/2$

As described in Section 5.2 the change of porosity between $T1$ and $T0$ has been estimated from the photogrammetric data, with $\Delta n=0.015$. The average porosity at $T1$ was estimated with $n1=0.28$, from a correlation of seismic velocities with porosity (Watkins et al., 1972). The elevation differences (Zs0−Zs1) refer to the data shown in Fig. 3. The thickness of the mass-movement (Zs0−Zsb) refers to the data shown in Fig. 10. The width of the flow channels $B$ was taken from Fig. 11.

Eq. (1) was converted to a finite difference equation and used to calculate the quantity $Q \cdot (T1-T0)$ at each cross-section shown in Fig. 11; this is the solid rock volume flowing through the plane of the section. The horizontal component of the mean displacement ($Dm$) through a vertical cross-section of the landslide mass ($S$) has been calculated by the following equation:

$$Dm = Q \cdot (T1-T0) \cdot (1-n1)^{-1} \cdot S^{-1} \quad (2)$$

The mean displacements ($Dm$) obtained by Eq. (2) have been associated with the centre flow lines of the flow channels. In a next step, these values were interpolated to the locations of the surface observations. Fig. 13 shows these calculated mean displacements together with the observed surface data, as well as the differences between the observed and calculated values. The average of all observed surface displacement data is 18.1 m, the average of the corresponding calculated values is 17.7 m. The average and standard deviation of the difference between these values are $\Delta=0.4\pm2.8$ m, which is not significant. Therefore, the rock mass exhibits a block movement and shear deformation is confined within the basal surface. The standard deviation of 2.8 m is only slightly higher than the estimated error of the data obtained by the photogrammetric method.

## 6. Conclusions

For the Gradenbach landslide area, aerial photographs from 1962 and 1996 have been processed by photogrammetric methods. This yields two digital terrain models and 51 displacement vectors for the mass-movement. For the 34 year interval, the average horizontal displacement component was 19±2.2 m and the vertical component was 11±2.1 m. The spatial distribution of the displacement values indicates a rather uniform movement. The difference between the two digital terrain models shows a significant decrease in height in the upper part and an increase in the lower part of the landslide. The total mass flux through vertical cross-sections has been calculated from these data and also an overall compaction of the creeping-mass of 1.5% has been inferred. Erosion has been estimated from the photogrammetric measurements at the toe of the slope. A kinematic interpretation of the photogrammetric data on the basis of the mass-movement thickness map, derived from geophysical measurements, resulted in information about the velocity depth profile. For the Gradenbach landslide, a block movement with high shear deformation at the basal shear zone or basal slip has been identified; this is of considerable importance for hazard estimates. The fit of the average velocities, derived from the two DTM and the geophysical thickness data, with the surface displacements is within the errors estimated for the photogrammetric method (<3 m).

The accuracy of the GPS displacement data is higher than that of the photogrammetric data by more than two orders of magnitude. Therefore, by using this method it has been possible to detect short-term variations in the velocities and also to show that these variations involve the whole mass-movement simultaneously, within a reaction time < 1 month. However, the strength of the photogrammetric measurements for the observation of the Gradenbach and similar mass-movements lies in the exploitation of the wealth of historical aerial photograph information obtained by earlier flights. Future work will show how to optimally combine photogrammetry and GPS, for the continued monitoring of the landslide and analysis of the surface displacement data sets.

## Acknowledgements

This paper is part of research projects funded by the Austrian Academy of Sciences within the Austrian contribution to IDNDR and ISDR. We would like to thank all colleagues who participated in the many strenuous field campaigns and who contributed to the

Please cite this article as: E. Brückl et al., Kinematics of a deep-seated landslide derived from photogrammetric, GPS and geophysical data, Engineering Geology (2006), doi:10.1016/j.enggeo.2006.09.004

analysis of the data. KAGIS provided the photogrammetric photos. We also thank the editors of this special issue and two anonymous reviewers for their valuable comments, which helped to improve the quality of the paper.

## References

Bisci, C., Dramis, F., Sorriso-Valvo, M., 1996. Rock flow (Sackung). In: Dikau, R., Brunsden, D., Schrott, L., Ibsen, M. (Eds.), Landslide Recognition. John Wiley & Sons, pp. 150–160.

Brückl, E., Brückl, J., 2006. Geophysical models of the Lesachriegel and Gradenbach deep-seated mass movements (Schober range, Austria). Engineering Geology 83, 254–272.

Brunner, F.K., Zobl, F., Gassner, G., 2003. On the capability of GPS for landslide monitoring. Felsbau (Rock and Soil Engineering) 21 (2), 51–54.

Casson, B., Delacourt, C., Baratoux, D., Allemand, P., 2003. Seventeen years of the "La Clapière" landslide evolution analysed from orthorectified aerial photographs. Engineering Geology 68, 123–139.

Finsterwalder, S., 1907. Die Theorie der Gletscherschwankungen. Zeitschrift für Gletscherkunde II, 81–103.

Isaaks, E., Srivastava, R.M., 1990. Applied Geostatistics. Oxford University Press, p. 580.

Kääb, A., 2002. Monitoring high-mountain terrain deformation from repeated air- and spaceborne optical data: examples using digital aerial imagery and ASTER data. ISPRS Journal of Photogrammetry and Remote Sensing 57, 39–52.

Kraus, K., Jansa, J., Kager, H., 1997. Photogrammetry, Volume 2: Advanced Methods and Applications. Dümmler, Bonn, p. 466.

Kraus, K., 2000. Photogrammetrie, Band 3: Topographische Informationssysteme. Dümmler, Bonn, p. 419.

Kraus, K., Pfeifer, N., 1998. Determination of terrain models in wooded areas with airborne laser scanner data. ISPRS Journal of Photogrammetry and Remote Sensing 53, 193–203.

KronfellnerKraus, G., 1980. Neue Untersuchungsergebnisse in Wildbächen — Der Talzuschub in Abhängigkeit von Niederschlägen. Int. Symp. Interpraevent Bad Ischl, vol. 1, pp. 179–192.

Mora, P., Baldi, P., Casula, G., Fabris, M., Ghirotti, M., Mazzini, E., Pesci, A., 2003. Global positioning systems and digital photogrammetry for the monitoring of mass movements: application to the Ca' di Malta landslide (northern Apennines, Italy). Engineering Geology 68, 103–121.

Nye, J.F., 1963. On the theory of advance and retreat of glaciers. Geophysical Journal of the Royal Astronomical Society 7 (4), 431–456.

Watkins, J.S., Walters, L.A., Godson, R.H., 1972. Dependence of in-situ compressional wave velocity on porosity in unsaturated rocks. Geophysics 37, 29–35.

Weidner, S., 2000. Kinematik und Mechanismus tiefgreifender alpiner Hangdeformationen unter besonderer Berücksichtigung der hydrologischen Verhältnisse. Dissertation, Friedrich–Alexander-Universität Erlangen–Nürnberg, 246.

Weidner, S., Moser, M., Lang, E., 1998. Influence of hydrology on sagging of mountain slopes ("Talzuschübe") — New results of time series analysis. 8th International IAEG Congress, Vancouver, Canada, Balkema, Rotterdam, pp. 1259–1266.

Wieser, A., Brunner, F.K., 2002. In: Adám, Schwarz (Eds.), SIGMA-F: Variances of GPS Observations Determined by a Fuzzy System, IAG Symposia, Vol. 125. Vistas for Geodesy in the New Millenium, pp. 365–370.

Zischinsky, U., 1969. Über Sackungen. Rock Mechanics 1, 30–52.

Please cite this article as: E. Brückl et al., Kinematics of a deep-seated landslide derived from photogrammetric, GPS and geophysical data, Engineering Geology (2006), doi:10.1016/j.enggeo.2006.09.004